Macromolecules
ARTICLE

Macromolecules **2009**, *42*, 4701–4711 **4701**
DOI: 10.1021/ma900640a

Complementary Multiple Hydrogen-Bonding Interactions Increase the Glass Transition Temperatures to PMMA Copolymer Mixtures

Shiao-Wei Kuo* and Hsin-Tung Tsai

Department of Materials and Optoelectronic Science, Center for Nanoscience and Nanotechnology, National Sun Yat-Sen University, Kaohsiung 804, Taiwan

Received March 25, 2009; Revised Manuscript Received May 13, 2009

ABSTRACT: We have prepared a series of poly(methyl methacrylate) (PMMA)-based copolymers through free radical copolymerizations of methyl methacrylate in the presence of the either 2-vinyl-4,6-diamino-1,3,5-triazine (VDAT) or vinylbenzylthymine (VBT). Using ^{1}H nuclear magnetic resonance (NMR) spectroscopy, solid state ^{13}C NMR spectroscopy, differential scanning calorimetry (DSC), one- and two-dimensional Fourier transform infrared (FTIR) spectroscopy, and viscosity measurements, we investigated the thermal properties of and hydrogen-bonding interactions within blends of the two copolymers poly(2-vinyl-4,6-diamino-1,3,5- triazine-*co*-methyl methacrylate) (PVDAT-*co*-PMMA) and poly(vinylbenzylthymine-*co*-methyl methacrylate) (PVBT-*co*-PMMA). A large positive deviation in the behavior of the glass transition temperature—determined using the Kwei equation and DSC analyses—indicated that strong multiple hydrogen-bonding interactions existed between the two copolymers. The FTIR and solid-state NMR spectroscopic analyses provided positive evidence for the presence of three hydrogen bonds between the diamino-1,3,5-triazine groups of PVDAT and thymine groups of PVBT. Furthermore, the proton spin−lattice relaxation time in the rotating frame [$T_{1\rho}$(H)] for the copolymer blends had a single value that was less than those of the pure copolymers, indicating that the degree of homogeneity of the D-PMMA/T-PMMA blend was relatively higher than those of the blends.

Introduction

Polymers possessing high glass transition temperatures are attractive materials in the polymer industry. For instance, poly(methyl methacrylate) (PMMA) is a colorless, commercially mass-produced, transparent polymeric material exhibiting high light transmittance, chemical resistance, and weathering corrosion resistance and good insulation.[1] These properties make PMMA a valuable substitute for glass in optical device applications, e.g., compact discs (CDs), optical glasses, and optical fibers.[2] Because the glass transition temperature of PMMA is, however, relatively low (T_g = ca. 100 °C), its applications in the optical-electronic industry are limited because it undergoes distortion when used in an inner glazing material.[3,4]

To raise the value of T_g, PMMA copolymers incorporating rigid or bulky monomer structures (to overcome the miscibility problem)[3,4] and monomers that can form hydrogen bonds with the carbonyl groups of PMMA have been reported widely.[5−10] Previously, we suggested an approach to raise the value of T_g of PMMA through copolymerization with methacrylamide (MAAM) because hydrogen-bonding interactions exist between these two monomer segments.[11,12] The values of T_g of such copolymers are generally higher than those of the corresponding polymer blends because, as it has been reported widely, compositional heterogeneities exist in hydrogen-bonded copolymers.[13,14] In all previous studies, the monomers have possessed relatively weak (single) hydrogen-bonding moieties (e.g., hydroxyl, carboxyl, pyridyl, or ether groups). Such intermolecular interactions must be present at relatively high mole percentages to enhance the thermal behavior of the copolymers; therefore, the structures of the copolymers differ substantially from those of their unmodified polymers.[15−17] Ideally, adding low mole percentages of the recognition units into the copolymers would enhance their thermal and mechanical properties.[18−29]

Complementary multiple hydrogen-bonding arrays play a fundamental role in complex biological systems (e.g., DNA duplexes). The self-assembly of pairs of DNA strands is mediated by intermolecular hydrogen bonding between complementary purine [adenine (A) and guanine (G)] and pyrimidine [thymine (T) and cytosine (C)] bases attached to a phosphate sugar backbone: G binds selectively to C, and A binds selectively to T.[30] Mimicking the molecular recognition by biological system is one of the most attractive themes in contemporary science.[31] Taking this cue from nature, we wondered whether we could enhance the thermal properties of PMMA by preparing synthetic polymers possessing nucleotide bases on their side chains. Komiyama et al. used free radical polymerization to prepare a series of copolymers based on 2-vinyl-4,6-diamino-1,3,5-triazine (VDAT),[32−34] which can form triply hydrogen-bonded complexes with thymine adducts in nonpolar solvents. A ^{1}H NMR spectroscopic titration experiment suggested that the interassociation equilibrium constant between diamino-1,3,5-triazine (DAT) and thymine (T) is ca. 890 M^{-1};[35] i.e., it is stronger than the interassociation equilibrium constant between A and T (ca. 530 M^{-1}).[36] As a result, we chose 2-vinyl-4,6-diamino-1,3,5-triazine (VDAT) and 1-(4-vinylbenzyl) thymine (VBT) as monomers for independent copolymerization with methyl methacrylate monomer, noting that VDAT and T have low self-association equilibrium constants (K_{dim} = ca. 2−3 M^{-1})[35,37] but form very strong complexes together (K_a = ca. 890 M^{-1}; Scheme 1).[35]

Poly(2-vinyl-4,6-diamino-1,3,5-triazine) (PVDAT) recognizes nucleic acid bases efficiently through three-point hydrogen bonding between 2,4-diaminotriazine and T units.[38] Therefore, we

*To whom corresponding should be addressed: e-mail kuosw@faculty.nsysu.edu.tw; Tel 886-7-5252000 ext 4079; Fax 886-7-5254099.

Published on Web 05/26/2009

expected that strong multiple hydrogen-bonding interactions would exist between the 2,4-diaminotriazine groups of the PVDAT units and the T groups of the poly(vinylbenzylthymine) (PVBT) units in blends of poly(2-vinyl-4,6-diamino-1,3,5-triazine-*co*-methyl methacrylate) (PVDAT-*co*-PMMA) and poly(vinylbenzylthymine-*co*-methyl methacrylate) (PVBT-*co*-PMMA). Fourier transform infrared (FTIR) spectroscopy—monitoring the stretching vibrations of these multiple hydrogen bonds—is an excellent probe for detecting molecular interactions between the components of polymers.[39,40] Solid-state nuclear magnetic resonance (NMR) spectroscopy is another powerful tool for monitoring specific interactions, miscibility, domain sizes, and molecular mobility resulting from hydrogen bond formation.[41−43] Furthermore, the spin−lattice relaxation time in the rotating frame [$T_{1\rho}$(H)] is sensitive to the mobilities of the local polymer chains; the domain size can also be estimated using spin-diffusion processes. In this study, we used differential scanning calorimetry (DSC) to examine the thermal properties of blends of PVDAT-*co*-PMMA and PVBT-*co*-PMMA featuring multiple hydrogen-bonding interactions; in addition, we used FTIR spectroscopy, solid-state NMR spectroscopy, and viscosity measurements to determine the effects of hydrogen bonding on the domain sizes and molecular motions.

Scheme 1. Formation of Strong Multiple Hydrogen-Bonding Interactions from between Diamino-1,3,5-triazine (DAT) and Thymine (T) Units

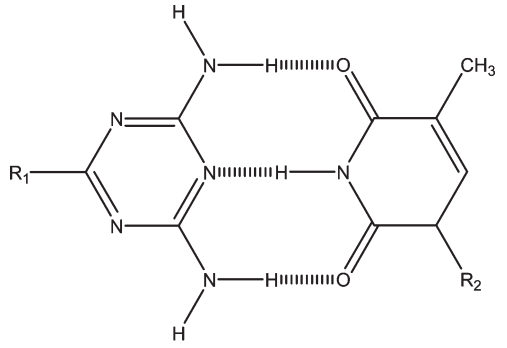

Ka = 890 M^{-1}

Experimental Section

Materials. Methyl methacrylate and thymine were purchased from the Aldrich Chemical Co.; they were purified through vacuum distillation and stored under a N_2 atmosphere prior to polymerization. Vinylbenzyl chloride was purchased from Acros Organics (Germany) and distilled prior to use. VDAT was purchased from Tokyo Kasei Kogyo Co. 2,2′-Azobis(isobutyronitrile) (AIBN) was recrystallized from methanol. Dimethylformamide (DMF) and dimethyl sulfoxide (DMSO) were distilled from CaH_2 under vacuum prior to use. All other chemicals were of reagent grade and used as received without further purification. VBT was prepared from thymine and vinylbenzyl chloride using a procedure described previously.[33]

Poly(vinylbenzylthymine-*co*-methyl methacrylate) (PVBT-*co*-PBMA) and Poly(2-vinyl-4,6-diamino-1,3,5-triazine-*co*-methyl methacrylate) (PVDAT-*co*-PMMA). The solution copolymerizations of methyl methacrylate with VDAT and VBT were performed in DMSO at 70 °C under an Ar atmosphere within glass reaction flasks equipped with condensers. AIBN was employed as the initiator; the mixtures were stirred for ca. 24 h. The products were dissolved in DMSO and then poured into excess MeOH under vigorous agitation to precipitate the copolymers. These two copolymers were characterized using ^{1}H NMR spectroscopy, FTIR spectroscopy, DSC, thermogravimetric analysis (TGA), and gel permeation chromatography (GPC). To determine the reactivity ratios, samples of the copolymers were taken from the reaction flasks during the early stages of copolymerization, i.e., when the degrees of conversion were low (4−9%). Scheme 2 outlines the synthetic procedures and the structures of the various components.

Blend Preparation. Blends of the copolymers PVDAT-*co*-PMMA and PVBT-*co*-PMMA were prepared through solution blending. DMF solutions containing 5 wt % of the polymer mixture were stirred for 6−8 h; the solvent was then left to

Scheme 2. Syntheses of PVDAT-*co*-PMMA and PVBT-*co*-PMMA Random Copolymers through Free Radical Polymerization

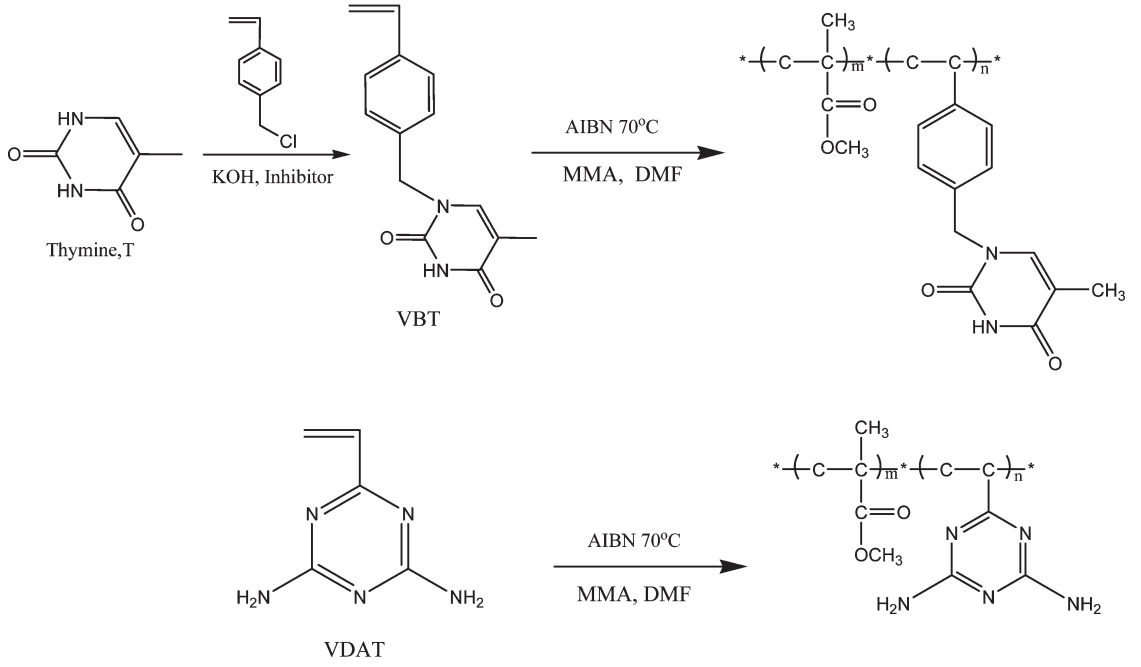

radical polymerization.

evaporate slowly at room temperature for 24 h. The resulting blend films were dried at 50 °C for 2 days.

Characterization. Molecular weights and molecular weight distributions were determined at 40 °C through GPC using a Waters 510 HPLC equipped with a 410 differential refractometer, a UV detector, and three Ultrastyragel columns (100, 500, and 10^3 Å) connected in series; DMF was the eluent; the flow rate was 0.6 mL/min. The molecular weight calibration curve was obtained using polystyrene (PS) standards. ^{1}H NMR spectra were obtained using an INOVA 500 instrument; acetone-d_6 was the solvent. The glass transition temperatures of the polymer blend films were determined through DSC using a TA Q-20 instrument. The scan rate was 20 °C/min within the temperature range 30−200 °C; the temperature was then held at 200 °C for 3 min to ensure complete remove of residual solvent. The values of T_g were measured in the DSC sample cell after the sample (5−10 mg) had been cooled rapidly to −50 °C from the melt of the first scan. The glass transition temperature was defined at the midpoint of the heat capacity transition between the upper and lower points of deviation from the extrapolated liquid and glass lines. FTIR spectra of the polymer blend films were recorded using the conventional KBr disk method. A DMF solution containing the blend was cast onto a KBr disk and dried under conditions similar to those used in the bulk preparation. The films used in this study were sufficiently thin to obey the Beer−Lambert law. FTIR spectra were recorded using a Bruker Tensor 27 FTIR spectrophotometer; 32 scans were collected at a spectral resolution 1 cm^{-1}. Because polymers containing VDAT and VBT groups are hygroscopic, pure N_2 gas was used to purge the spectrometer's optical box to maintain dry sample films. Generalized 2D correlation analysis was performed using the 2D Shige software developed by Shigeaki Morita (Kwansei-Gakuin University, Japan). In the 2D correlation maps, white regions are defined as positive correlation intensities; shaded regions are defined as negative correlation intensities. High-resolution solid-state ^{13}C NMR spectra were recorded at room temperature using a Bruker DSX-400 spectrometer operated at resonance frequencies of 399.53 and 100.47 MHz for ^{1}H and ^{13}C spectra, respectively. The ^{13}C CP/MAS spectra were measured using a 90° pulse of 3.9 μs, a pulse delay time of 3 s, and an acquisition time of 30 ms; a total of 2048 scans were collected. All NMR spectra were recorded at 300 K using broadband proton decoupling and a normal cross-polarization pulse sequence. A magic angle spinning (MAS) rate of 5.4 kHz was used for the sample to avoid overlapping of absorptions. The value of $T_{1\rho}$(H) was determined indirectly through carbon atom observation using a 90°−τ−spin-lock pulse sequence prior to cross-polarization. The data acquisition was performed through ^{1}H decoupling with delay times (τ) ranging from 0.1 to 10 ms and a contact time of 1.0 ms.

Results and Discussion

Analyses of Copolymers. VDAT and VBT are soluble in most common solvents. Figure 1 presents ^{1}H NMR spectra of VDAT and the copolymer PVDAT-*co*-PMMA in d_6-DMSO. For VDAT, we observe the two doublets and quartet typical of a vinyl group (1$\mathbf{H}_b$, 1$\mathbf{H}_a$, and 2$\mathbf{H}_c$,) at 5.66, 6.32, and 6.41 ppm with a relative mole ratio of 1:1:1, corresponding to the iso, trans, and substituted vinyl protons, respectively. The amino (NH_2) group appears as a signal located at 6.68 ppm. The signals of the vinylic hydrogen atoms of VDAT are absent in the spectrum of D20-PMMA (i.e., the D-PMMA copolymer containing 20 mol % of VDAT), indicating that the starting monomers had been removed completely. We estimated the mole percentage of VDAT from the ratio of the integrals of the amino ($\mathbf{H}_d$) protons of VDAT and the OCH_3 ($\mathbf{H}_a$ = 3.55 ppm) protons of MMA. Similarly, the spectrum of VBT (Figure 2a) displays two doublets and a quartet resonance typical of a vinyl group (1$\mathbf{H}_b$, 1$\mathbf{H}_a$, and 2$\mathbf{H}_c$,) at 5.26, 5.77, and 6.98 ppm with a relative mole ratio of 1:1:1; the resonances of the T unit's CH_3 ($\mathbf{H}_h$) and benzylic CH_2 ($\mathbf{H}_f$) groups appear at a mole ratio of 3:2 at 1.80 and 4.87 ppm, respectively; the NH unit of the T group appears as a signal at 11.30 ppm. Figure 2b presents the ^{1}H NMR spectrum of T12-PMMA (i.e., the T12-PMMA copolymer containing 12 mol % of VBT). The signals of the vinylic hydrogen atoms of VBT are absent, indicating that the starting monomers were removed completely. We estimated the mole percentage of VBT from the ratio of the integrals of benzylic ($\mathbf{H}_f$) protons of VBT and the OCH_3 ($\mathbf{H}_a$) protons of MMA. Table 1 lists the monomer feed ratios and resultant copolymer compositions from which we calculated the reactivity ratios (r_{VDAT} = 1.12 and r_{MMA} = 0.38; r_{VBT} = 12.04 and r_{MMA} = 1.39)

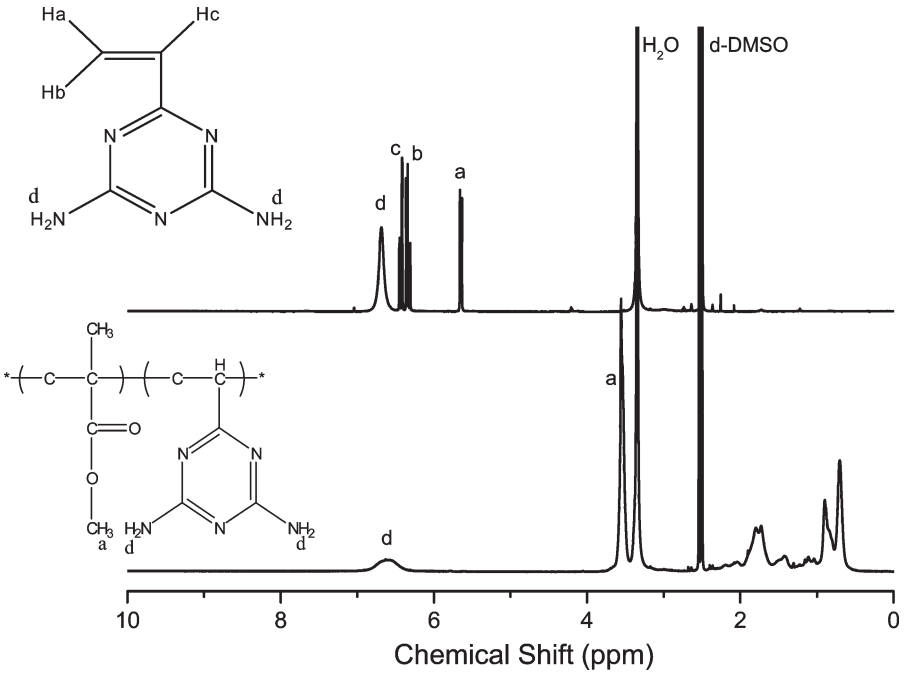

Figure 1. ^{1}H NMR spectra of VDAT and PVDAT-*co*-PMMA copolymers in d_6-DMSO at room temperature.

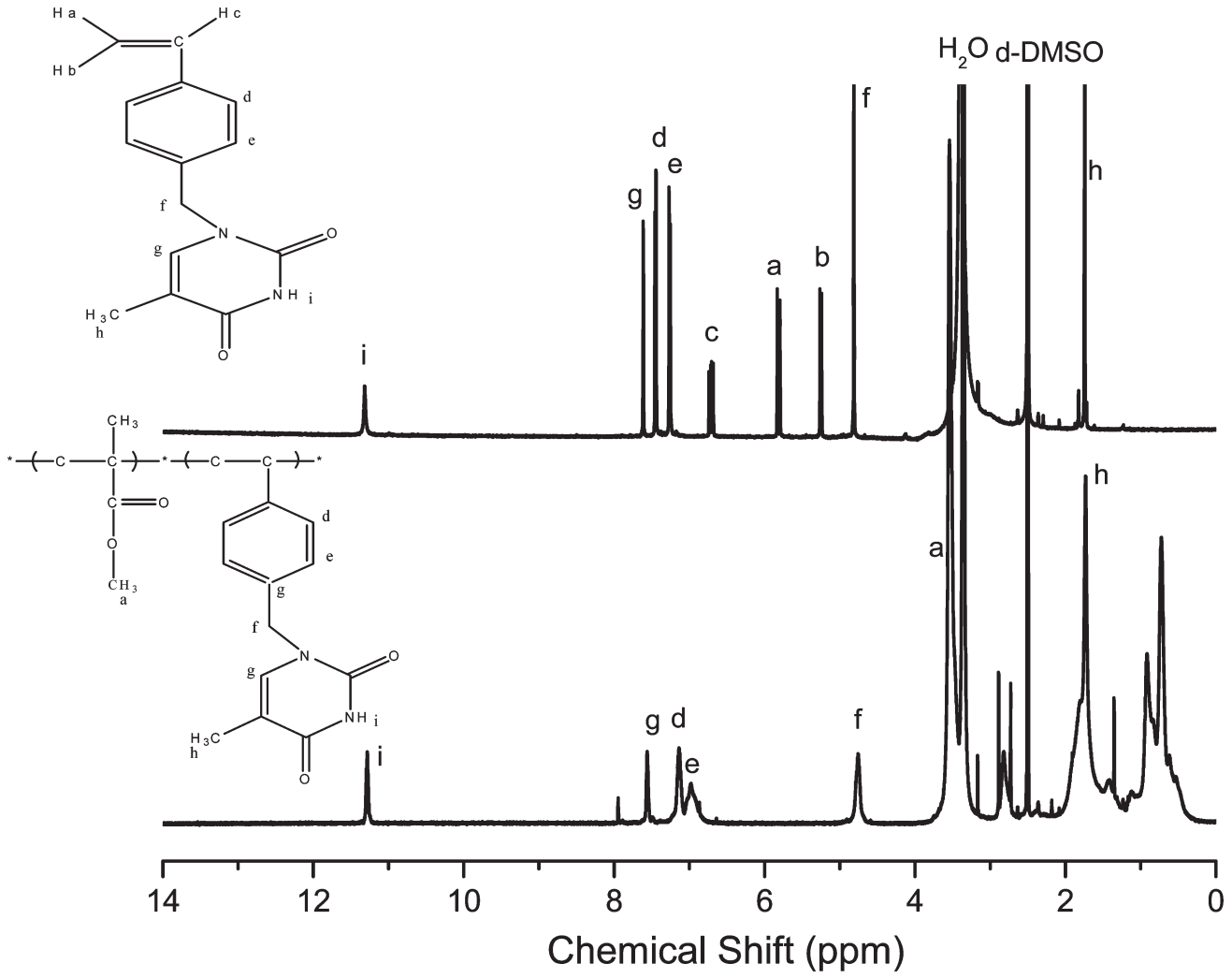

Figure 2. ^{1}H NMR spectra of VBT and PVBT-*co*-PMMA copolymers in d_6-DMSO at room temperature.

Table 1. Properties of the PVDAT-*co*-PMMA and PVBT-*co*-PMMA Copolymers

sample	feed (VBT/MMA)	copolymer[a] (PVDAT/PMMA)	M_w[b]	M_n[b]	PDI[b]	T_g[c] (°C)	T_d[d] (°C)
pure PMMA	0:100	0:100	42 200	25 800	1.63	100	352
T01-PMMA	1.2:98.8	0.9:99.1	37 700	24 300	1.55	103	353
T02-PMMA	2.2:97.8	2.1:97.9	36 200	22 500	1.61	111	366
T05-PMMA	4.4:95.6	5.4:94.6	41 100	22 400	1.83	114	381
T12-PMMA	9.4:90.6	12.1:87.9	33 500	21 400	1.56	125	407
sample	feed (VDAT/MMA)	copolymer[a] (PVDAT/PMMA)	M_w[b]	M_n[b]	PDI[b]	T_g[c] (°C)	T_d[d] (°C)
D05-PMMA	2.2:97.8	4.7:95.3	63 900	47 300	1.35	116	347
D09-PMMA	3.6:96.4	8.5:91.5	87 000	60 000	1.45	119	357
D14-PMMA	7.5:92.5	14.4:85.6	91 100	61 500	1.48	133	361
D20-PMMA	15.4:84.6	19.5:80.5	88 400	59 400	1.49	139	350

[a] Estimated from ^{1}H NMR. [b] Relative molecular weights against polystyrene standard calculated from GPC in THF. [c] Determined by DSC at 20 °C/min. [d] Determined by TGA at 20 °C/min.

using the methodology of Kelen and Tudos, as discussed previously;[44] these values indicate that these two copolymers were essentially random copolymers with a tendency toward blocky structures.

Figure 3 displays FTIR spectra (room temperature) of PVDAT-*co*-PMMA copolymers incorporating various VDAT compositions. The NH stretching of DAT appears as signals located at 3487, 3372, and 3204 cm^{-1} (symmetric and asymmetric stretching vibrations); additional signals appear at 1614 and 1574 cm^{-1} (phenyl breathing) and 1550 cm^{-1} (C=N stretching).[45,46] Clearly, the intensities of the absorptions of this DAT group at 1510−1670 and 3100−3600 cm^{-1} increased upon increasing the VDAT fraction in the copolymers. Figure 4 displays FTIR spectra (room temperature) of PVBT-*co*-PMMA copolymers featuring various VBT compositions. The intensity of the absorption of the thymine C=O group at ca. 1688 cm^{-1} increased upon increasing the VBT fraction in the copolymer. In addition, the signal of the free C=O groups of PMMA appears at 1730 cm^{-1}; this peak did not undergo any chemical shifts upon increasing the PVDAT or PVBT contents, indicating that no specific interactions existed between the C=O groups

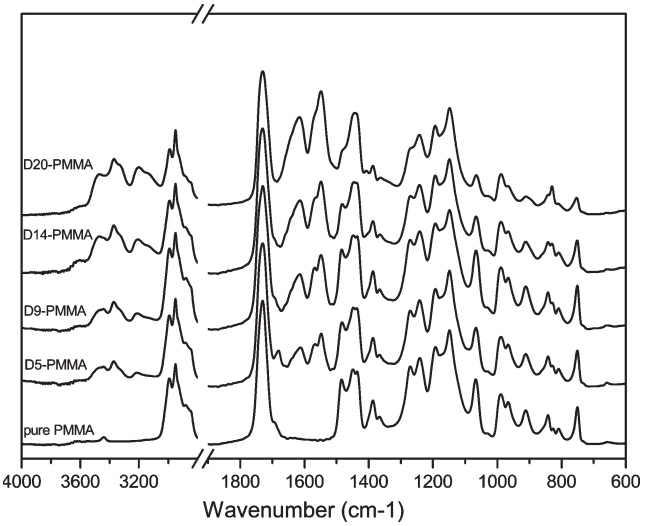

Figure 3. FTIR spectra of PVDAT-*co*-PMMA copolymers recorded at room temperature.

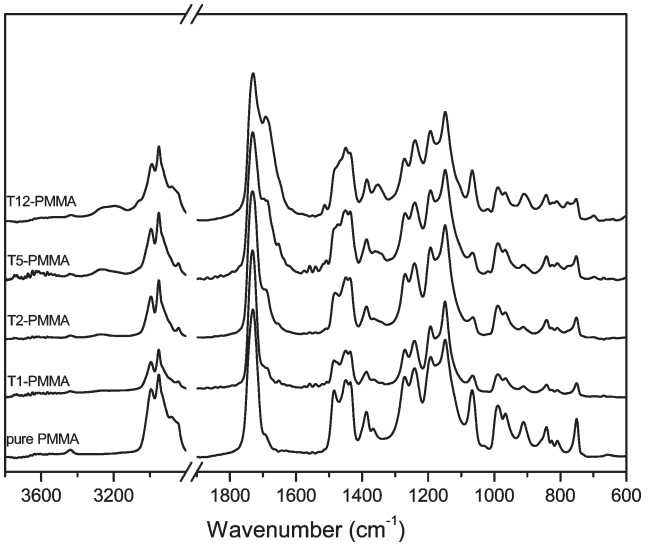

Figure 4. FTIR spectra of PVBT-*co*-PMMA copolymers recorded at room temperature.

of PMMA and either the DAT groups of PVDAT or the T groups of PVBT.

Figure 5 displays DSC curves, recorded at temperatures ranging from 0 to 180 °C, of the PVDAT-*co*-PMMA and PVBT-*co*-PMMA copolymers. Pure PMMA exhibits a single glass transition temperature at ca. 100 °C; the glass transition temperatures of the two copolymers increased upon increasing their VDAT and VBT contents, with the Fox equation revealing a positive deviation. In addition, the thermal decomposition temperatures also increased significantly upon increasing the contents of these nucleobases. Table 1 summarizes the monomer feed ratios, compositions, molecular weights, glass transition temperatures, and thermal decomposition temperatures of the synthesized copolymers. In terms of nomenclature, the descriptor T12-PMMA, for example, represents a copolymer containing 12 mol % of VBT.

Copolymer Blend. A single value of T_g detected by DSC is conventionally employed as a criterion reflecting the miscibility of a polymer blend. Figure 6 displays DSC thermograms of PVDAT-*co*-PMMA/PVBT-*co*-PMMA 50/50 blends, where the D-PMMA and T-PMMA components contain various contents of VDAT and VBT, respectively. Each of these binary blends exhibited a single glass transition

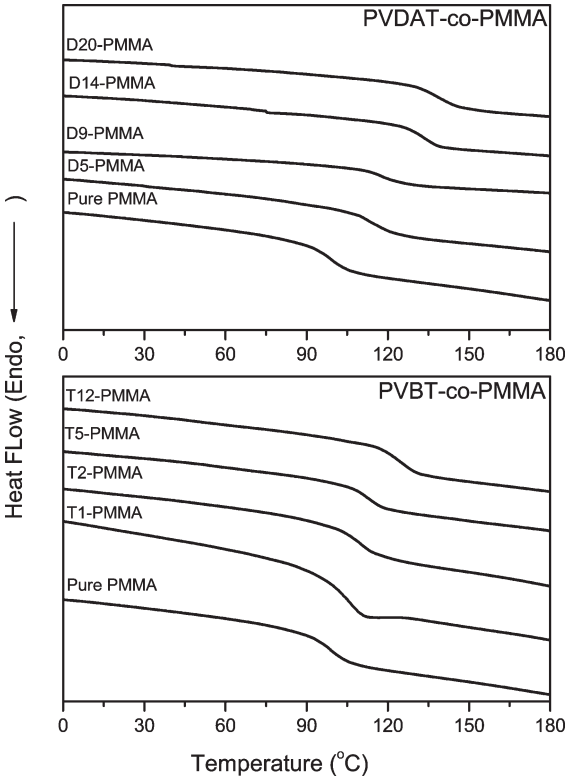

Figure 5. DSC thermograms of PVDAT-*co*-PMMA and PVBT-*co*-PMMA copolymers.

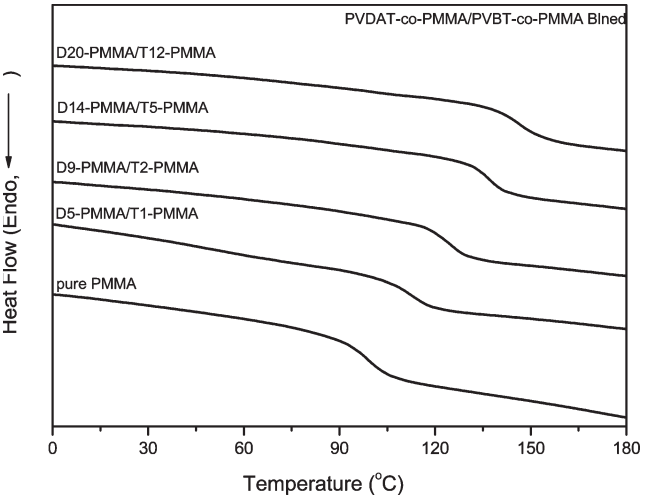

Figure 6. DSC thermograms of D-PMMA/T-PMMA binary blends.

temperature, indicating that the blends were miscible on the range 20−40 nm; the value of T_g shifted upon increasing the VDAT or VBT content in these two PMMA-based copolymers. It is notable that blending only 12 mol % of VBT and 20 mol % of VDAT into the PMMA copolymer chain increased the value of T_g by 50 °C relative to that of pure PMMA, providing a glass transition temperature similar to that of polycarbonate.

Over the years, a number of empirical equations have been offered to predict the variations in glass transition temperatures of miscible blends and diblock copolymers as a function of composition. The Kwei equation[47] is usually employed for systems displaying specific interactions:

$$T_g = \frac{W_1 T_{g1} + kW_2 T_{g2}}{W_1 + kW_2} + qW_1 W_2 \quad (1)$$

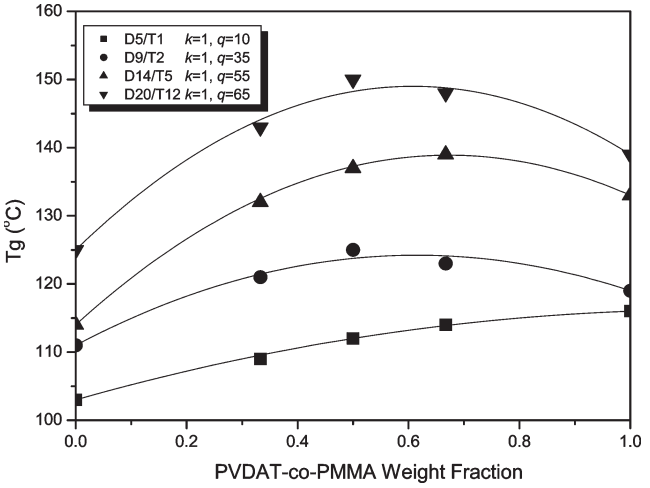

Figure 7. Plots of T_g with respect to composition, based on the Kwei equation.

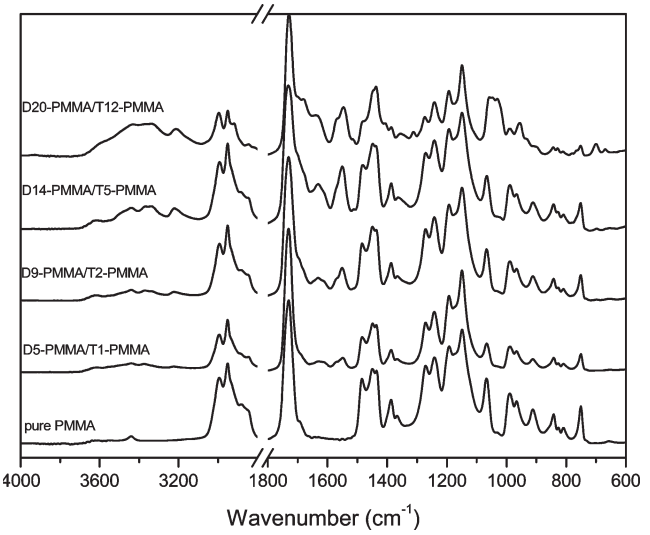

Figure 8. FTIR spectra of D-PMMA/T-PMMA blends incorporating various VDAT and VBT contents, recorded at room temperature.

where w_1 and w_2 are the weight fractions of the components, T_{g1} and T_{g2} are the corresponding glass transition temperatures, and k and q are fitting constants. The parameter q corresponds to the strength of specific interactions in the system, reflecting a balance between the breaking of the self-association interactions and the forming of the interassociation interactions. Figure 7 illustrates the dependence of T_g on the composition of the PVDAT-*co*-PMMA/PVBT-*co*-PMMA blends incorporating various VDAT and VBT contents. The values of q increased upon increasing the VDAT and VBT contents in the PMMA copolymer main chain; for the D20-PMMA/T12-PMMA blend system, we obtained the largest value ($q = 65$), implying that this blend system featured stronger multiple hydrogen bonds than did the other three copolymer blends because of the presence of a larger number of nucleic acid base units.

FTIR Spectroscopic Analyses. Infrared spectroscopy is a highly effective means of investigating the specific interactions between polymers. It can be used as a tool to study, both qualitatively and quantitatively, the mechanism of interpolymer miscibility through the formation of hydrogen bonds. Figure 8 displays FTIR spectra recorded at room temperature for the PVDAT-*co*-PMMA/PVBT-*co*-PMMA copolymer blends containing various mole percentages of VDAT and VBT units. The NH vibration of DAT appears as signals located at 3424 and 3540 cm^{-1}, corresponding to symmetric and asymmetric stretch vibrations, respectively.[35] For VDAT units incorporated into the PMMA main chain, the absorption shifted because the DAT groups were distributed randomly in the PMMA, and therefore, the probability of self-associative hydrogen bonding of the VDAT groups was low because of the diluent effect in the hydrogen-bonding system.[48,49] In Figure 9a it is clear that the DAT groups interacted with the T group—the absorptions shifted to 3338 and 3462 cm^{-1}. In addition, a peak appeared at 3216 cm^{-1} that corresponded to the NH group in T interacting with a DAT group.[35] Figure 9b displays FTIR spectra (1500−1800 cm^{-1}) recorded at room temperature for D20-PMMA blended with the T12-PMMA copolymer. The position of the signal for the free C═O groups of PMMA (1730 cm^{-1}) did not change after blending, implying the PMMA units did not form any hydrogen bonds with the VDAT and VBT units. As mentioned above, the absorptions at ca. 1688 and 1616 cm^{-1} are due to the T and DAT groups, respectively (Figure 9b). We also observe two new peaks at ca. 1677 cm^{-1} (C═O group of T interacting with DAT) and 1632 cm^{-1} (DAT group interacting with NH group of T). The changes are caused by multiple hydrogen bond formation between the DAT units and the imide groups of the T units.[50]

Figure 10 presents scale-expanded FTIR spectra of D20-PMMA/T12-PMMA 50/50 blends recorded at various temperatures. The peaks corresponding to C−H stretching (2800−3000 cm^{-1}) and to vibration of the free C═O groups of PMMA (1730 cm^{-1}) did not change upon increasing the temperature. In contrast, all of the peaks associated with the multiple hydrogen-bonding interactions shifted to higher wavenumbers—except for that of the DAT group at 1616 cm^{-1}, which shifted to lower wavenumber, consistent with the destruction of a hydrogen bond of a pyridine group[51]—indicating that heat disrupted these noncovalent interactions. At temperatures higher than the value of T_g of the blend, a new peak appeared at ca. 1600 cm^{-1}, corresponding to a free NH_2 scissor vibration plus a ring stretching vibration of the VDAT group, indicating that the multiple hydrogen-bonding interactions between the DAT and T groups had become disrupted.

We used two-dimensional (2D) correlation spectroscopy to further characterize the interactions in this blend system. This approach has been applied widely in polymer science[52−55] as a novel method for investigating the specific interactions between polymer chains by treating the spectral fluctuations as a function of time, temperature, pressure, and composition. White and shadow areas in 2D IR correlation contour maps represent positive and negative cross-peaks, respectively. The 2D synchronous spectra are symmetric with respect to the diagonal line in the correlation map. Auto peaks, which represent the degree of autocorrelation of perturbation-induced molecular vibrations, are located at the diagonal positions of a synchronous 2D spectrum; their values are always positive. When an auto peak appears, the signal at that wavenumber would change greatly under environmental perturbation. Cross-peaks located at off-diagonal positions of a synchronous 2D spectrum (they may be positive or negative) represent the simultaneous or coincidental changes of the spectral intensity variations measured at v_1 and v_2. Positive cross-peaks result when the intensity variations of the two peaks at v_1 and v_2 occur in the same direction (i.e., both increase or both decrease) under the environmental perturbation; negative cross-peaks reveal that the intensities of the two peaks at v_1 and v_2 change in

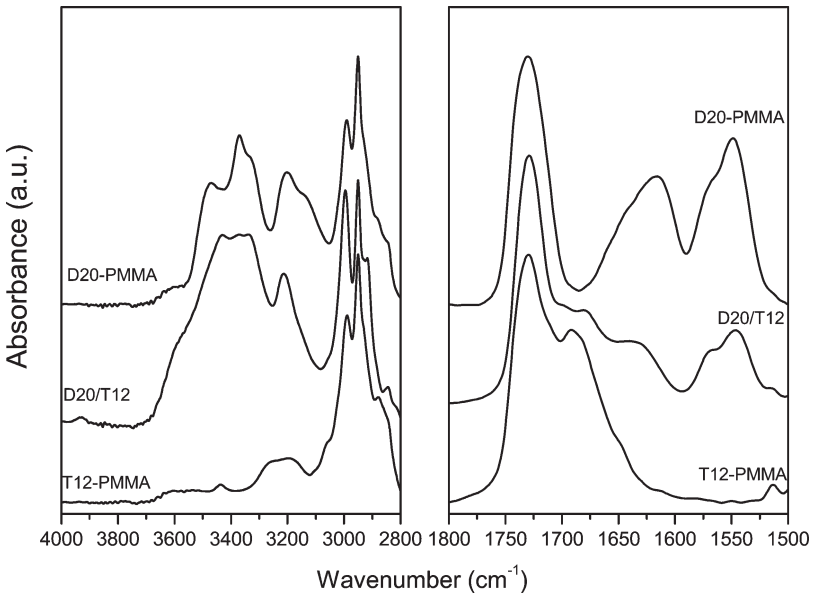

Figure 9. FTIR spectra of D20-PMMA, T12-PMMA, and their corresponding blends, recorded at room temperature.

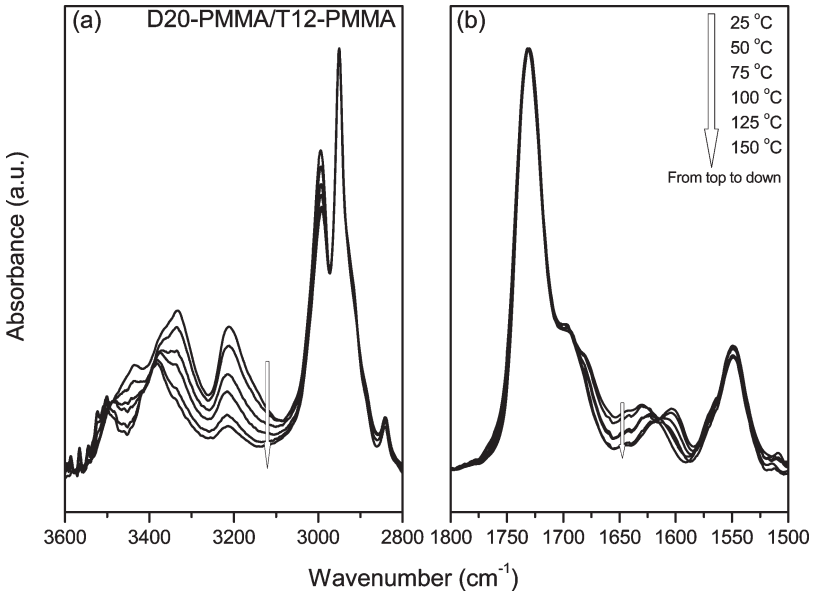

Figure 10. FTIR spectra of D20-PMMA/T12-PMMA blends, recorded at various temperatures.

opposite directions (i.e., one increases while the other decreases) under perturbation.[55]

Figure 11a presents synchronous 2D IR correlation maps recorded in the range 1550−1780 cm^{-1}. The absorption bands in this spectral range that are associated with PVBT-*co*-PMMA copolymers appear at 1740 cm^{-1} (free C═O groups of PMMA) and 1677 cm^{-1} (hydrogen-bonded C═O groups of T units). The signals associated with PVDAT-*co*-PMMA appear at 1600 cm^{-1} for the free triazine units and at 1630 cm^{-1} for the hydrogen-bonded VDAT groups. Two positive cross-peaks existed for this system: (1600 vs 1740) and (1632 vs 1677). These positive cross-peaks all changed in the same direction (according to Noda's rule) upon increasing the temperature. Four negative cross-peaks appeared at (1600 vs 1632), (1600 vs 1677), (1632 vs 1740), and (1677 vs 1740); i.e., these four bands vary in the opposite direction. Although two hydrogen-bonded or two free groups should undergo changes in the same direction, we would expect the free functional groups to vary in the opposite direction to that of the hydrogen-bonded functional groups. Figure 11b provides an analysis of the signals in the regions 1550−1780 and 3000−3600 cm^{-1}, which represent the signals for the NH stretching bands, to provide a macroscopic view of the interactions. Clearly, the signs of the cross-peaks in the synchronous maps for the hydrogen-bonded groups at 3216, 3338, and 3462 cm^{-1} are positive with respect to the hydrogen-bonded groups at 1632 and 1677 cm^{-1}, but they are negative with respect to the free C═O groups at 1740 and 1600 cm^{-1}; these results confirmed our previous assignments.

Solid-State NMR Spectroscopic Analyses. Evidence for interactions within the blends can also be obtained from solid-state NMR spectroscopy, as demonstrated by changes in chemical shifts and/or line shapes.[56] Figure 12 presents selected ^{13}C CP/MAS spectra of various T12-PMMA and D20-PMMA copolymers and the T12-PMMA/D20-PMMA 50/50 blend. We observe signals for the **C**−NH_2 units of D20-PMMA at 168.0 ppm, the **C**═O units of the T groups of T12-PMMA at 164.0 and 151.1 ppm, respectively, and the

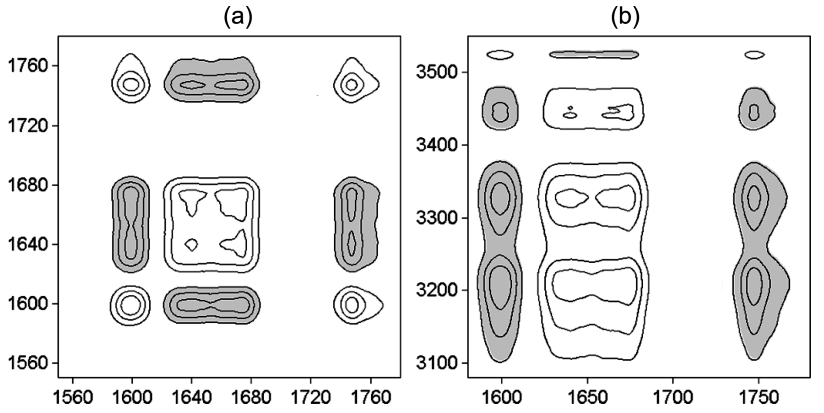

Figure 11. (a) Synchronous 2D IR correlation maps for the region from 1550 to 1780 cm^{-1}. (b) Synchronous 2D correlation maps for the regions from 1550 to 1780 cm^{-1} and from 3100 to 3600 cm^{-1} for D20-PMMA/T12-PMMA blends under temperature perturbation.

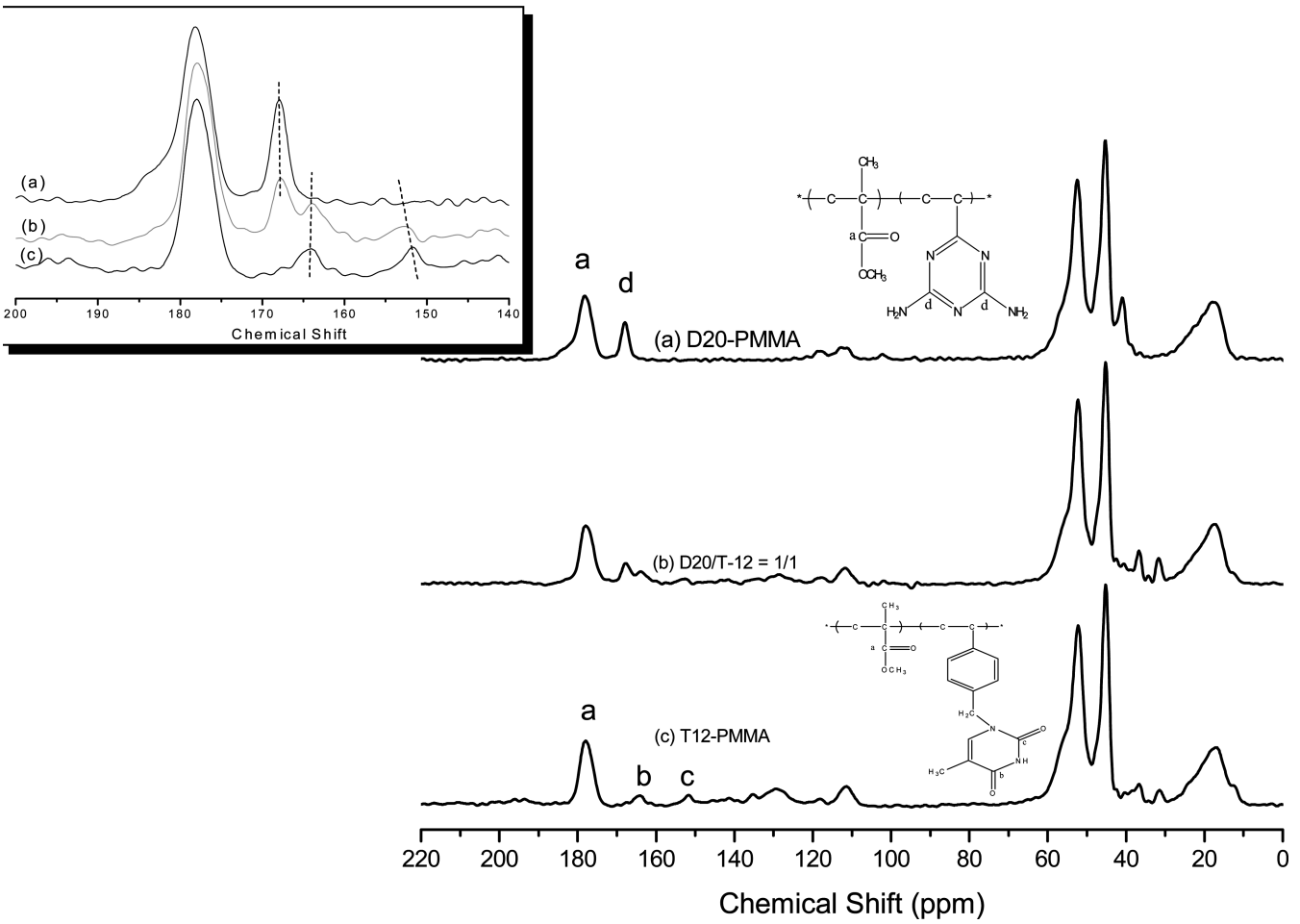

Figure 12. ^{13}C CP/MAS NMR spectral data for D20-PMMA, T12-PMMA, and their corresponding blend at room temperature.

C═O units of PMMA at 178.0 ppm. Further evidence for hydrogen bonding in the DAT:VBT blend was provided by the ^{13}C NMR spectroscopic data, which displayed a upfield shift (0.2 ppm) for the aromatic carbon atom of DAT and a downfield shift (0.1−0.5 ppm shift) for the signal of the C═O unit of VBT.

Solid-state NMR spectroscopy can also be used to determine the phase behavior and miscibility of blends. A single value of T_g, based on DSC analysis, implies that the mixing of two blend components occurs on a scale of ca. 20−40 nm. The dimension of mixing smaller than 20 nm can be obtained through measurement of the spin−lattice relaxation time in the rotating frame ($T_{1\rho}^{H}$).[40] We measured the values of $T_{1\rho}^{H}$ of the diblock copolymers and blend complex through delayed-contact ^{13}C CP/MAS experiments, using the equation $M_\tau = M_0 \exp[-\tau/T_{1\rho}(H)]$, where τ is the delay time used in the experiment and M_τ is the corresponding resonance intensity. Figure 13 presents plots of $\ln(M_\tau/M_0)$ with respect to τ for the signal at 45 ppm of D20-PMMA, T12-PMMA, and their blend. The experimental data are in good agreement with calculated values. The slope of the fitting line provides the value of $T_{1\rho}^{H}$. Table 2 lists these values for the pure copolymers and the blend. We obtained a single composition-dependent value of $T_{1\rho}^{H}$ for each of the copolymers and their

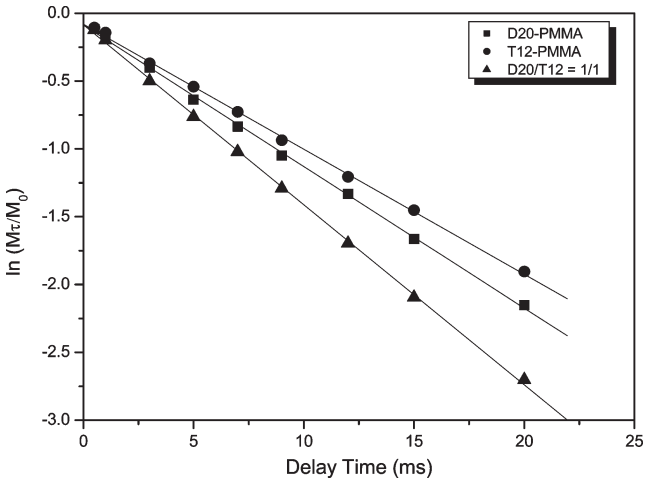

Figure 13. Logarithmic plots of the intensities of 45 ppm for PMMA with respect to the delay time.

Table 2. Relaxation Times $T_{1\rho}^{H}$ for D20-PMMA, T12-PMMA, and Their Blends at Magnetization Intensities of 17, 45, and 52 ppm

samples	17 ppm	45 ppm	52 ppm
D20-PMMA	10.85	9.84	9.58
T12-PMMA	10.54	10.54	10.84
D20-PMMA/T12-PMMA = 1/1	7.96	7.21	7.53

blend, suggesting that they are homogeneous on the scale at which the spin diffusion occurs within the time $T_{1\rho}^{H}$. The upper spatial scale of the spin-diffusion path length L can be estimated using the equation[40] $L = (6DT)^{1/2}$, where D (typically 10^{-16} m^2 s^{-1}) is the effective spin-diffusion coefficient depending on the average proton-to-proton distance as well as the dipolar interaction (Table 2). In addition, the value of $T_{1\rho}^{H}$ for the blend was lower than those of the two pure copolymers. These results imply that the copolymer mixtures featuring multiple hydrogen-bonding interactions have relatively smaller domain sizes than those of the corresponding pure copolymers, indicating that the degree of homogeneity of the D20-PMMA/T-12PMMA copolymer was relatively higher than those of the blends. On the basis of our DSC, solid-state NMR spectroscopy, and FTIR spectroscopy analyses, we conclude that the multiple hydrogen-bonding interactions in the PVDAT-*co*-PMMA/PVBT-*co*-PMMA blends led to complex aggregation behavior.

We further characterized this copolymer mixture by using an Ubbelohde viscometer to measure the solution viscosity of a mixture of D20-PMMA and T12-PMMA in THF. The formation of supramolecular polymers in the D20-PMMA/T12-PMMA blends provided a higher solution viscosity relative to that of pure PMMA as shown in Figure 14; in addition, the viscosity increased upon increasing the concentrations of the copolymers. This supramolecular polymer also could be observed macroscopically—in the form of a gel—from a 1:1 mixture of D20-PMMA/T12-PMMA in THF at a concentration of 30 g/dL; at the same concentration, a solution of PMMA, which lacked any specific interpolymer hydrogen-bonding interactions, flowed freely (see the inset to Figure 14). Scheme 3 shows the possible chain behaviors of D-PMMA/T-PMMA blends through multiple hydrogen bonding units into PMMA, which enchanced the thermal properties and dramatically increased the viscosity as a result of the formation of supramolecular polymers.

Interassociation Equilibrium Constant Analyses. Painter and Coleman[57,58] suggested adding an additional term—accounting for the free energy of hydrogen bond formation—to a simple Flory−Huggins expression for the free energy of mixing of two polymers:

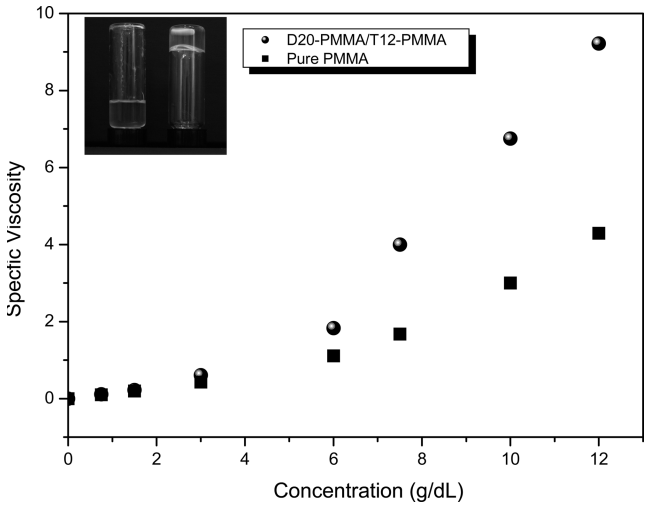

Figure 14. Plots of specific viscosity of D20-PMMA/T12-PMMA blend and pure PMMA in THF solution vs concentration. Inset: photographs of the corresponding blends at the same concentration (of 30 g/dL).

Table 3. Self- and Interassociation Equilibrium Constants and Thermodynamic Parameters for PVDA-*co*-PMMA/PVBT-*co*-PMMA Blends at 25 °C[a]

polymer	molar volume (mL/mol)	molecular weight (g/mol)	δ (cal/mL)$^{1/2}$	equilibrium constant K_B	equilibrium constant K_A
PMMA	84.9	100	9.1		
PVDAT	122.1	133.1	12.0	18.0	
PVBT	161.7	242.1	12.1		7300
D20-PMMA	462	537	9.9	18.0	
T12-PMMA	784	975	9.7		7300

[a] δ: solubility parameter; K_B: self-association equilibrium constant; K_A: interassociation equilibrium constant.

$$\frac{\Delta G_N}{RT} = \frac{\Phi_1}{N_1}\ln\Phi_1 + \frac{\Phi_2}{N_2}\ln\Phi_2 + \Phi_1\Phi_2\chi_{12} + \frac{\Delta G_H}{RT} \quad (2)$$

where Φ and N are the volume fraction and the degree of polymerization, respectively, χ is the "physical" interaction parameter, the subscripts 1 and 2 define the two blend components, and ΔG_H is the free energy change contributed by hydrogen bonding between the two components. According to the Painter−Coleman equation, the relative magnitude of the inter- and self-association equilibrium constants, rather than their individual absolute values, is the most important factor when determining the dominant contributions to the free energy of mixing. In general, the interassociation equilibrium constant K_A is calculated from either the polymer blend system or a low-molecular-weight model compound.[63] In our system, pure PVDAT and PVBT dissolve only in high-polarity solvents, such as DMF and DMSO, which interfere with self- and interassociation hydrogen bonding and would, therefore, provide incorrect equilibrium constants.[57] Thus, we use the interassociation equilibrium constants (K_a) of low-molecular-weight model compounds—2,4-diamino-6-dodecyltriazine and *N*-1-propylthymine—to determine the interassociation equilibrium constant (K_a = 890 M^{-1}), based on an approach described previously by Beijer et al.[32] We transformed the value of K_a for the model compound into K_A by dividing by the molar volume of the VDAT repeat unit (0.121 L mol^{-1} at 25 °C),[57]

providing a value for the interassociation equilibrium constant K_A of 7300. Likewise, by dividing the value of K_b of 2.2 M^{-1} for the model compound 2,4-diamino-6-dodecyltriazine by the molar volume of the VDAT repeat unit, we determined that the self-association equilibrium constant (K_B) of VDAT was 18.[32] To minimize errors, we ignored the self-association of T groups because the T−T interaction is almost the same strength as the DAT−DAT interaction;[35,37] furthermore, two self-associating, hydrogen-bonded donor polymer blend systems would make analysis of the binary blend system too complicated.[59,60]

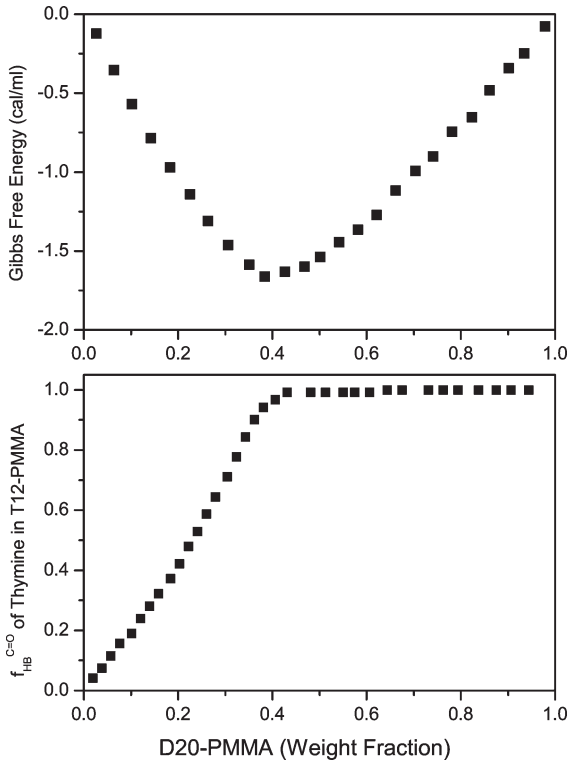

Figure 15. (a) Calculated free energies of mixing for D20-PMMA/T12-PMMA blends of various compositions at 25 °C and (b) theoretical fractions of hydrogen-bonded C=O groups of T units in the T12-PMMA copolymer at 25 °C.

Although we did not obtain these interassociation equilibrium constants from polymer mixtures, the standard interassociation equilibrium constant of the polymer blend could be calculated from the low-molecular-weight model compound mixtures by considering the intramolecular screening effect and functional group accessibility.[57] The intramolecular screening effect is a consequence of chain connectivity. The covalent linkage between polymer segments causes an increase in the number of same-polymer-chain contacts as a result of the polymer chains bending back on themselves; thus, the number of interassociation hydrogen bonds per unit volume in the polymer blend will be lower than that for the model compound. For an infinite chain, γ is surprisingly large, approaching 0.38 in the melt state; for real chains, however, the value is closer to 0.3.[61] Moreover, the spacing between the functional groups along a polymer chain and the presence of bulky side groups can also significantly reduce the interassociation hydrogen bonding per unit volume, as a result of a so-called functional group accessibility effect.[48] This effect is also considered to be the origin of steric crowding and shielding.[62] Table 3 lists all the parameters required by the PCAM to estimate the thermodynamic properties for these polymer blends. Here, we emphasize the thermodynamic properties of only the D20-PMMA/T12-PMMA copolymer mixtures. On the basis of FTIR and solid-state NMR spectroscopic analyses, we knew that the position of signal for the free C=O groups of PMMA did not change after blending, implying that the PMMA segments did not form hydrogen bonds with the VDAT and VBT units. As a result, the PMMA segment can be considered as an inert diluent.[48,61,62] Table 3 also summarizes the

Scheme 3. Schematic Representation of the Supramolecular Network Structure Formed from PMMA Copolymer Mixtures Featuring Specific Multiple Hydrogen-Bonding Interactions

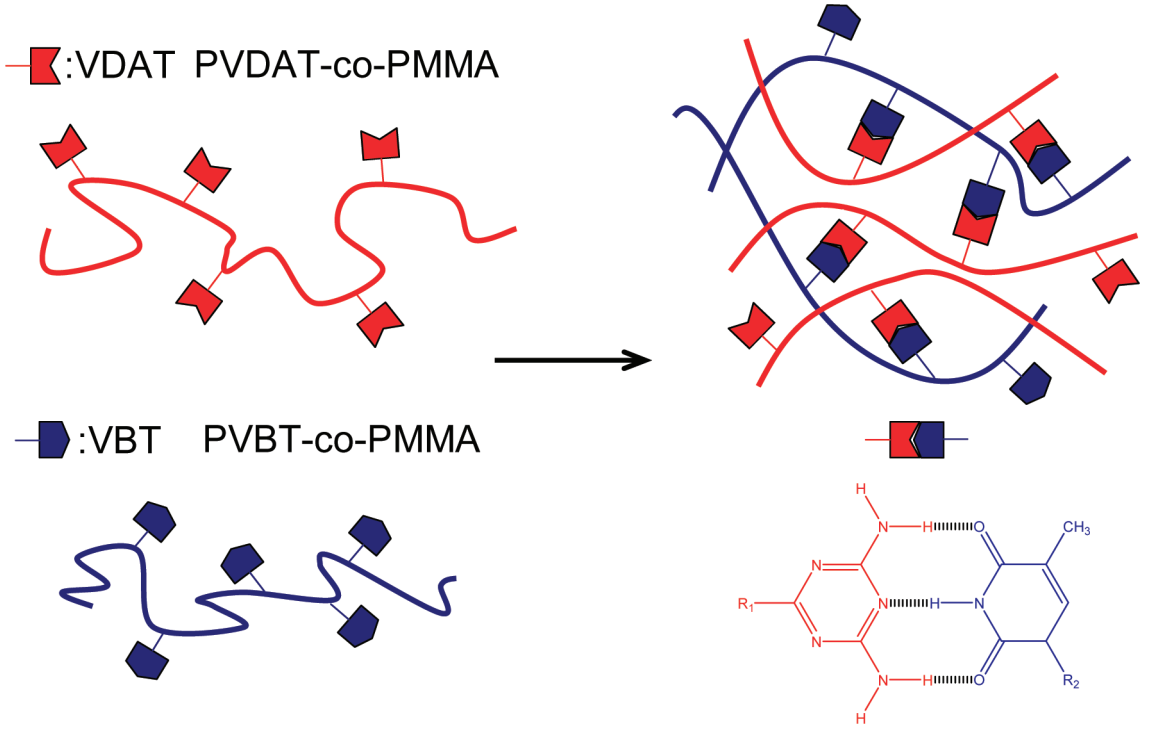

corresponding molecular volumes, molecular weights, and solubility parameters of these blends.

We performed the calculation of Gibbs free energy of binary D20-PMMA/T12-PMMA blend and fraction of hydrogen-bonded carbonyl of T using the Miscible Polymer Blend Calculator Software package.[57] The approach used to correlate the hydrogen-bonding equilibrium concentration to the free energy values has been described previously.[62] Figure 15a reveals that the predicted free energy (ΔG_m) of the D20-PMMA/T12-PMMA blend was negative for all compositions at room temperature. The value of ΔG_m reached a minimum of -1.7 cal/cm^3 when the PVDAT content was ca. 40 wt %; we can consider the D20-PMMA/T12-PMMA blend to be miscible because of the negative free energy and the positive second derivative of the weight fraction over the entire range of compositions. Figure 15b presents plots of the theoretically predicted curves with respect to the composition at room temperature; the fraction of hydrogen-bonded C=O group of T unit reached 100% when the PVDAT content was ca. 40 wt %.

Conclusions

We have used free radical polymerization to synthesize nucleobase (DAT and T)-functionalized PMMA random copolymers. Incorporating these multiple hydrogen-bonding units into PMMA enhanced the thermal properties and dramatically increased the viscosity as a result of the formation of supramolecular polymers. We observed a positive deviation of the dependence of T_g on the polymer composition, based on the Kwei equation, owing to strong hydrogen bonding existing between the PVDAT-*co*-PMMA and PVBT-*co*-PMMA copolymer main chains. FTIR and solid-state NMR spectroscopic analyses both provided positive evidence for hydrogen-bonding interactions within these copolymer systems. We obtained a single value of the spin−lattice relaxation times in the rotating frame for the copolymer blend that was lower than those of the pure copolymers, suggesting a decrease in the free volume of the blend. Thus, significant increases in the value of T_g of PMMA can be achieved through copolymerization of methyl methacrylate individually with complementary nucleobase monomers and then mixing of the resulting copolymers to form multiple hydrogen-bonding interactions.

Acknowledgment. This work was supported financially by the National Science Council, Taiwan, Republic of China, under Contracts NSC 97-2221-E-110-013-MY3 and NSC 97-2120-M-009-003.

References and Notes

(1) Yuichi, K. *J. Appl. Polym. Sci.* **1997**, *63*, 363.
(2) Kine, B. B.; Novak, R. W. In *Encyclopedia of Polymer Science and Engineering*, 2nd ed.; Kroschwitz, J. L., Ed.;Wiley: New York, 1986; Vol. 1, p 234.
(3) Otsu, T.; Motsumoto, T. *Polym. Bull.* **1990**, *23*, 43.
(4) Braun, D.; Czerwinski, W. K. *Makromol. Chem.* **1987**, *188*, 2389.
(5) Mishra, A.; Sinha, T. M. J.; Choudhary, V. *J. Appl. Polym. Sci.* **1998**, *68*, 527.
(6) Dong, S.; Wang, Q.; Wei, Y.; Zhang, Z. *J. Appl. Polym. Sci.* **1999**, *72*, 1335.
(7) Tagaya, A.; Harada, T.; Koike, K.; Koike, Y.; Okamoto, Y.; Teng, H.; Yang, L. *J. Appl. Polym. Sci.* **2007**, *106*, 4219.
(8) Cornejo-Barvo, J. M.; Siegel, R. A. *Biomaterials* **1996**, *17*, 1167.
(9) Chauhan, R.; Choudhary, V. *J. Appl. Polym. Sci.* **2009**, *112*, 4088.
(10) Teng, H.; Koike, K.; Zhou, D.; Satoh, Z.; Koike, Y. *J. Polym. Sci., Part A: Polym. Chem.* **2009**, *47*, 315.
(11) Kuo, S. W.; Kao, H. C.; Chang, F. C. *Polymer* **2003**, *44*, 6873.
(12) Chen, J. K.; Kuo, S. W.; Kao, H. C.; Chang, F. C. *Polymer* **2005**, *46*, 2354.
(13) Coleman, M. M.; Xu, Y.; Painter, P. C. *Macromolecules* **1994**, *27*, 127.
(14) Kuo, S. W.; Xu, H.; Huang, C. F.; Chang, F. C. *J. Polym. Sci., Polym. Phys.* **2002**, *40*, 2313.
(15) Kuo, S. W. *J. Polym. Res.* **2008**, *15*, 459.
(16) Zhuang, H. F.; Perace, E. M.; Kwei, T. K. *Macromolecules* **1994**, *27*, 6398.
(17) Chen, S. C.; Kuo, S. W.; Liao, C. S.; Chang, F. C. *Macromolecules* **2008**, *41*, 8865.
(18) IIhan, F.; Gray, M.; Rotello, V. M. *Macromolecules* **2001**, *34*, 2597.
(19) Xu, H.; Norsten, T. B.; Uzum, O.; Jeoung, E.; Rotello, V. M. *Chem. Commun.* **2005**, *41*, 5157.
(20) Feldman, K. E.; Kade, M. J.; de Greef, T. F. A.; Meijer, E. W.; Kramer, E. J.; Hawker, C. J. *Macromolecules* **2008**, *41*, 4694.
(21) Seo, M.; Beck, B. J.; Paulusse, J. M. J.; Hawker, C. J.; Kim, S. Y. *Macromolecules* **2008**, *41*, 6413.
(22) Sivakava, S.; Wu, J.; Campo, C. J.; Mather, P. J.; Rowan, S. J. *Chem.—Eur. J.* **2006**, *12*, 446.
(23) Hofmeier, H.; Schubert, U. S. *Chem. Commun.* **2005**, *19*, 2423.
(24) Park, P.; Zimmerman, S. C. *J. Am. Chem. Soc.* **2006**, *128*, 11582.
(25) Mather, B. D.; Baker, M. B.; Beyer, F. L.; Berg, M. A. G.; Green, M. D.; Long, T. E. *Macromolecules* **2007**, *40*, 6834.
(26) Nair, K. P.; Breedveld, V.; Weck, M. *Macromolecules* **2008**, *41*, 3429.
(27) Mather, B. D.; Lizotte, J. R.; Long, T. E. *Macromolecules* **2004**, *37*, 9331.
(28) Bazzi, H. S.; Sleiman, H. F. *Macromolecules* **2002**, *35*, 9617.
(29) Park, P.; Zimmerman, S. C. *J. Am. Chem. Soc.* **2006**, *128*, 14236.
(30) Watson, J. D.; Berry, A. *DNA: The Secret of Life*; Knopf: New York, 2003.
(31) Smith, J. R. *Prog. Polym. Sci.* **1996**, *21*, 209.
(32) Asanuma, H.; Ban, T.; Gotoh, S.; Hishiya, T.; Komiyama, M. *Macromolecules* **1998**, *31*, 371.
(33) Asanuma, H.; Ban, T.; Gotoh, S.; Hishiya, T.; Komiyama, M. *Supramol. Sci.* **1998**, *5*, 405.
(34) Asanuma, H.; Ban, T.; Gotoh, S.; Hishiya, T.; Komiyama, M. *J. Chem. Soc., Perkin Trans.* **1998**, *2*, 1915.
(35) Beijer, F. H.; Sijbesma, R. P.; Vekemans, J. A. J. M.; Meijer, E. M.; Kooijman, H.; Spek, A. L. *J. Org. Chem.* **1996**, *61*, 6371.
(36) Kuo, S. W.; Cheng, R. S. *Polymer* **2009**, *50*, 177.
(37) Kyogoku, Y.; Lord, R. C.; Rich, A. *J. Am. Chem. Soc.* **1967**, *89*, 496.
(38) Sherrington, D. C.; Taskinen, K. A. *Chem. Soc. Rev.* **2001**, *30*, 83.
(39) Coleman, M. M.; Graf, J. F.; Painter, P. C. *Specific Interactions and the Miscibility of Polymer Blends*; Technomic Publishing: Lancaster, PA, 1991.
(40) Kuo, S. W.; Chang, F. C. *Macromolecules* **2001**, *34*, 5224.
(41) Hill, D. J. T.; Whittaker, A. K.; Wong, K. W. *Macromolecules* **1999**, *32*, 5285.
(42) Zhang, X.; Takegoshi, K.; Hikichi, K. *Macromolecules* **1992**, *25*, 2336.
(43) Jack, K. S.; Whittaker, A. K. *Macromolecules* **1997**, *30*, 3560.
(44) Kelen, T.; Tudos, F. *J. Macromol. Sci., Chem.* **1975**, *A9*, 1.
(45) Ariga, K.; Kamino, A.; Koyano, H.; Kunitake, T. *J. Mater. Chem.* **1997**, *7*, 1155.
(46) Padgett II, a W. M.; Hamner, W. F. *J. Am. Chem. Soc.* **1958**, *80*, 803.
(47) Kwei, T. *J. Polym. Sci., Polym. Lett. Ed.* **1984**, *22*, 307.
(48) Pehlert, G. J.; Painter, P. C.; Veytsman, B.; Coleman, M. M. *Macromolecules* **1997**, *30*, 3671.
(49) Kuo, S. W.; Chang, F. C. *J. Polym. Sci., Polym. Phys.* **2002**, *40*, 1661.
(50) Beijer, F. H.; Kooijman, H.; Spek, A. L.; Sijbesma, R. P.; Meijer, E. W. *Angew. Chem., Int. Ed.* **1998**, *37*, 75.
(51) Kuo, S. W.; Lin, C. L.; Chang, F. C. *Polymer* **2002**, *43*, 3943.
(52) Noda, I. *J. Am. Chem. Soc.* **1989**, *111*, 8116.
(53) Kuo, S. W. *Polymer* **2008**, *49*, 4420.
(54) Kuo, S. W.; Lee, H. F.; Haung, W. J.; Jeong, K. U.; Chang, F. C. *Macromolecules* **2009**, *42*, 1619.
(55) Noda, I.; Ozaki, Y. *Two-Dimensional Correlation Spectroscopy*; John Wiley & Sons: New York, 2004.
(56) Damodaran, K.; Sanjayan, G. J.; Rajamohanan, P. R.; Ganapathy, S.; Ganesh, K. N. *Org. Lett.* **2001**, *3*, 1921.
(57) Coleman, M. M.; Painter, P. C. *Miscible Polymer Blend-Background and Guide for Calculations and Design*; DEStech Publications: Lancaster, PA, 2006.
(58) Painter, P. C.; Coleman, M. M. *Prog. Polym. Sci.* **1995**, *20*, 1.
(59) Park, Y.; Veytsman, B.; Coleman, M. M.; Painter, P. C. *Macromolecules* **2005**, *38*, 3703.
(60) Kuo, S. W.; Chan, S. C.; Wu, H. D.; Chang, F. C. *Macromolecules* **2005**, *38*, 4729.
(61) Painter, P. C.; Veytsman, B.; Kumar, S.; Shenoy, S.; Graf, J. F.; Xu, Y.; Coleman, M. M. *Macromolecules* **1997**, *30*, 932.
(62) Pehlert, G. J.; Painter, P. C.; Coleman, M. M. *Macromolecules* **1998**, *31*, 8423.